

Crystallization and Melting Behavior of Poly(*p*-phenylene sulfide) in Blends with Poly(ether sulfone)

MITSUHIRO SHIBATA,¹ RYUTOKU YOSOMIYA,¹ ZHENHUA JIANG,² ZHENZHONG YANG,² GUIBIN WANG,² RONGTANG MA,² ZHONGWEN WU²

¹ Department of Industrial Chemistry, Chiba Institute of Technology, 2-17-1, Tsudanuma, Narashino, Chiba 275-0016, Japan

² Department of Chemistry, Jilin University, 119, Jiefang Road, Changchun, 130023, China

Received 26 February 1999; accepted 12 April 1999

ABSTRACT: Crystallization and melting behaviors of poly(*p*-phenylene sulfide) (PPS) in blends with poly(ether sulfone) (PES) prepared by melt-mixing were investigated by differential scanning calorimetry (DSC). The blends showed two glass transition temperatures corresponding to PPS- and PES-rich phases, which increased with increasing PES content, indicating that PPS and PES have some compatibility. The cold crystallization temperature of the blended PPS was a little higher than that of pure PPS. Also, the heats of crystallization and melting of the blended PPS decreased with increasing PES content, indicating that the degree of crystallinity decreased with an increase of PES content. The isothermal crystallization studies revealed that the crystallization of PPS is accelerated by blending PPS with 10 wt % PES and further addition results in the retardation. The Avrami exponent n was about 4 independent on blend composition. The activation energy of crystallization increased by blending with PES. The equilibrium melting point decreased linearly with increasing PES content. © 1999 John Wiley & Sons, Inc. *J Appl Polym Sci* 74: 1686–1692, 1999

Key words: crystallization behavior; melting behavior; compatibility; poly(*p*-phenylene sulfide); poly(ether sulfone)

INTRODUCTION

Poly(*p*-phenylene sulfide) (PPS) is a high-performance thermoplastic polymer that is finding increasing use as either filled or unfilled molding resin.¹ The mechanical properties and morphology of semicrystalline PPS are highly dependent on the processing condition that governs the crystallization process.^{2,3} The crystallization behavior of PPS is found to be highly influenced by the presence of the second components such as inor-

ganic or organic fillers^{4–6} and other thermoplastics.^{7–12} Regarding the blends with thermoplastics, for example, the isothermal crystallization of PPS was accelerated in the blends with a liquid crystalline polyesteramide¹¹ and poly(ethylene terephthalate),¹² whereas it was retarded in the blends with high-density polyethylene.¹²

Poly(ether sulfone) (PES) is an amorphous high-performance engineering plastics with superior thermal (high glass transition temperature) and mechanical properties. Zeng and Yang investigated the crystallization kinetics of PPS/PES blends prepared by solution-mixing, reporting that the crystallization of PPS was retarded by the existence of PES and the Avrami exponent of the blends was lower than that of pure PPS.¹³

Correspondence to: M. Shibata.

Contract grant sponsor: National Science Foundation of China; contract grant number: 59433072.

Journal of Applied Polymer Science, Vol. 74, 1686–1692 (1999)

© 1999 John Wiley & Sons, Inc.

CCC 0021-8995/99/071686-07

In the present article, the crystallization and melting behavior of PPS/PES blends prepared by melt-mixing were studied in detail by differential scanning calorimetry (DSC). The influence of PES on the crystallization of PPS was evaluated by the use of the Avrami equation for the isothermal crystallization process, the equilibrium melt point estimated by Hoffman–Weeks method,¹⁴ and the total activity energy of crystallization estimated by Arrhenius equation.

EXPERIMENTAL

Materials

PES was kindly supplied by Nahu Chemical Industry Plant of Jilin University (Changchun, Jilin, China). The inherent viscosity was 0.38 dL/g. PPS used was a commercial grade P-3 manufactured by Sichuan Factory of High Performance Engineering (Chongqing, Sichuan, China).

Sample Preparation

The polymers were dried at 120°C in a vacuum oven for at least 24 h before use. Blending of PPS and PES was performed under a nitrogen atmosphere by using a 60-mL mixer attached to a Brabender-like apparatus. The molten mixing was carried out at 300°C, mixing speed was 64 rpm, and mixing time was 8 min. The blank PPS used for comparison was also subjected to the same treatment. The flat sheets of 0.2-mm thickness were prepared by compression molding, followed by quenching into ice water. Discs were cut from the sheets for DSC measurement.

Characterization

The melting behavior and the nonisothermal crystallization behaviors were characterized in a nitrogen atmosphere by a Perkin–Elmer DSC-7 apparatus, calibrated with zinc standard. The heating and cooling runs were always carried out at a rate of 10°C/min. The traces of the first heating run were recorded from 30 to 320°C. After holding the specimens at 320°C for 5 min to destroy the crystalline nuclei completely, the cooling traces were recorded from 320 to 30°C, and then the second heating scan was recorded. Isothermal crystallization experiments were carried out with the same apparatus. The samples were placed in DSC pans and heated to 310°C at a rate of 20°C/min, held for 5 min at that temperature, and then

cooled to the appropriate T_c at a rate of 200°C/min. The heat generated during the development of the crystalline phase was recorded until no further heat evolution was observed and analyzed according to the usual procedure to obtain the relative degree of crystallinity. The relative degree of crystallinity as a function of time was found from eq. (1),

$$\chi_c(t)/\chi_c(\infty) = \int_{t_0}^t (dH/dt)dt / \int_{t_0}^{\infty} (dH/dt) dt \quad (1)$$

where t_0 is the time at which the sample attains isothermal conditions, as indicated by a flat baseline after the initial spike in the thermal curve, $\chi_c(t)$ is the degree of crystallinity at time t , $\chi_c(\infty)$ is the ultimate crystallinity at a very long time, and dH/dt is the heat flow rate. At the end of each isothermal experiment, the samples were reheated at a heating rate of 10°C/min, for measuring the melting temperature.

RESULTS AND DISCUSSION

Nonisothermal Crystallization and Melting Behavior

The DSC thermograms of PPS and PES are shown in Figure 1. The first heating run of quenched PPS showed a glass transition temperature related to PPS (T_{g1}) at 84°C, a cold crystallization temperature (T'_c) at 120°C, and a melting temperature (T_m) at 274°C (curve b). In the cooling trace, a crystallization peak (T_c) was observed at 238°C, but no peak related to the glass transition was observed (curve c). The second heating run showed no cold crystallization exotherm (curve a), indicating that PPS crystallized completely during the 10°C/min cooling run. Regarding PES, a glass transition temperature-related PES (T_{g2}) was observed approximately at 219°C both in the heating and cooling runs (curve d and e).

The DSC thermograms of the PPS/PES (80/20) blend are shown in Figure 2. The first heating run showed all the transition peaks related to the PPS- and PES-rich phases except for T_{g2} (T_{g1} at 87°C, T'_c at 124°C, and T_m at 274°C, curve b). The cooling run of the blend showed a crystallization peak (T_c) at 236°C. In the second heating run, two glass transitions (T_{g1} at 91°C, T_{g2} at 190°C) were observed, and no crystallization peak related to PPS (T'_c) was observed (curve a). All the

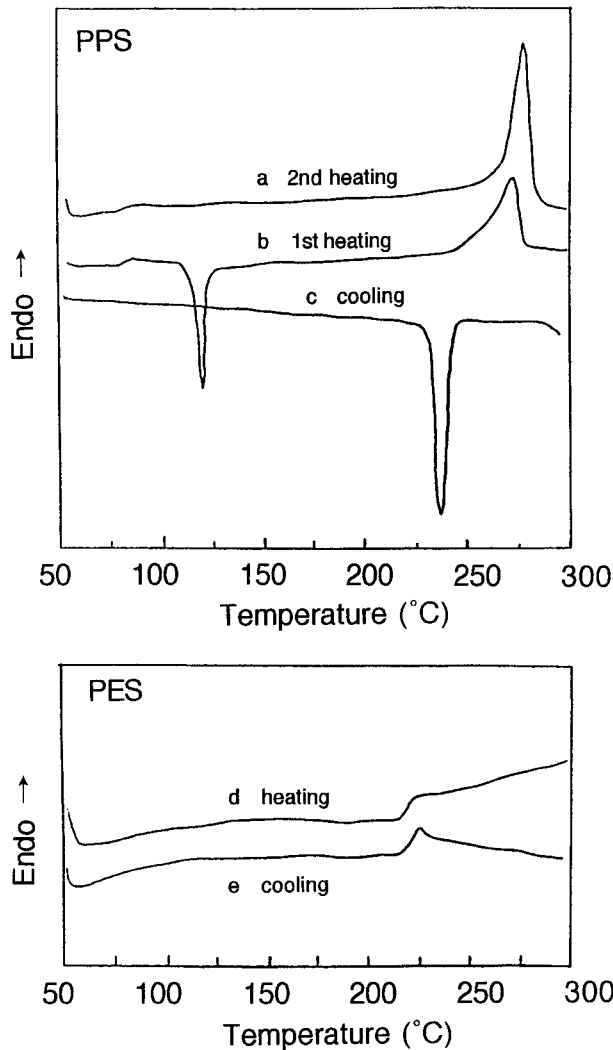


Figure 1 DSC thermograms of PPS and PES.

T_g , T_c , T'_c , and T_m for PPS, PES, and PPS/PES blend are summarized in Table I and II.

Although detectable glass transition related to PPS was not observed for the blends with PPS content $\leq 70\%$, the blends with PPS content $\geq 80\%$ showed the clear transition, and the T_{g1} increased with increasing PES content. On the other hand, T_{g2} decreased with increasing PPS content. The inward shift of the glass transition temperatures suggests that PPS and PES have some compatibility. The T'_c in the blends was a little higher than that of pure PPS. It is thought that the cold crystallization of PPS is somewhat disturbed by the increase of T_{g1} of the PPS-rich phase.

In the nonisothermal crystallization of PPS in blends with PES from melt at a cooling rate of

10°C , the onset temperature (T_{co}) and the peak temperature of crystallization (T_c) were little affected by the PES content, whereas the completion temperature of crystallization (T_{cc}) increased with increasing PES content. Consequently, the crystallization peak width ($T_{co} - T_{cc}$) decreased with increasing PES content. Also, the heat of crystallization (H_c) normalized to the PPS content decreased slightly with increasing PES content, indicating that the degree of crystallinity of PPS was lowered a little.

On the other hand, the peak temperature and completion temperature of melting (T_m and T_{mc}) vary little with composition, whereas the onset temperature of melting (T_{mo}) increased with increasing PES content. Consequently, the melting peak width ($T_{mc} - T_{mo}$) decreased with increasing PES content. The heat of fusion (H_m), normalized to the PPS content of the blends, decreased with increasing PES content. These results also indicate that the degree of crystallinity of PPS decreases with increasing PES content. Also, the H_m in the second heating run was higher than that in the first heating run, indicating that a higher crystallinity is attained in the crystallization from melt than in cold crystallization.

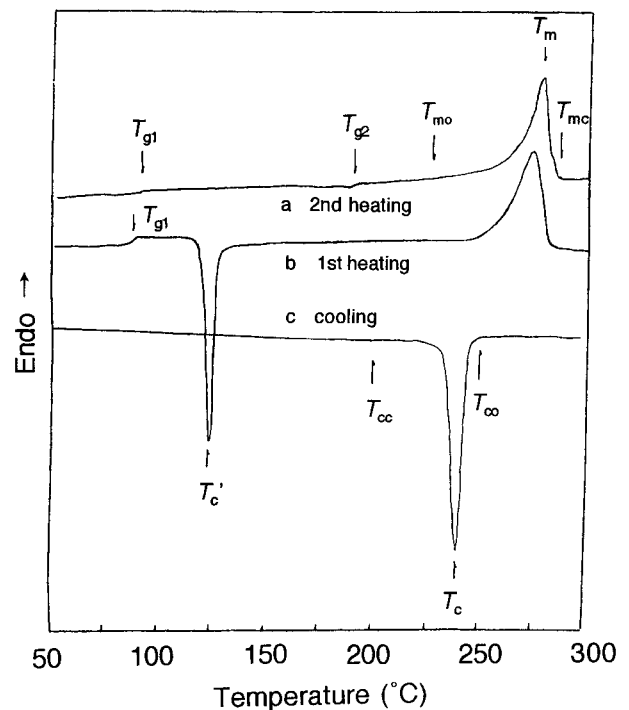


Figure 2 DSC thermograms of PPS/PES (80/20) blend.

Table I Calorimetric Data for PPS/PES Blends

Sample (PPS/PES)	T_{g1} (°C)	T_{g2} (°C)	T'_c (°C)	T_{mo} (°C)	T_m (°C)	T_{mc} (°C)	$T_{mo} - T_{mc}$ (°C)	H_m (J/g)
100/0								
1st heating	83.8	—	120.1	220.5	273.5	282.7	51.0	47.7
2nd heating	88.7	—	—	219.0	276.4	292.3	57.4	48.7
90/10								
1st heating	85.7	—	122.3	224.0	272.6	284.5	48.6	40.3
2nd heating	90.9	—	—	220.5	276.6	288.7	56.1	46.6
80/20								
1st heating	86.6	—	123.7	230.0	274.0	284.7	44.0	37.3
2nd heating	91.2	190.4	—	228.3	278.2	288.6	49.9	40.5
70/30								
1st heating	—	195.5	124.0	233.8	273.6	284.2	39.8	36.7
2nd heating	—	196.1	—	233.0	276.8	284.7	43.8	39.5
30/70								
1st heating	—	215.7	124.3	244.7	273.4	283.7	28.7	35.5
2nd heating	—	213.7	—	243.7	273.4	281.7	29.7	37.0
20/80								
1st heating	—	217.4	124.0	240.7	273.7	284.5	33.0	33.3
2nd heating	—	215.2	—	242.8	273.9	282.7	31.1	38.6
10/90								
1st heating	—	218.2	120.7	246.7	273.5	284.5	26.8	33.8
2nd heating	—	218.2	—	246.7	273.6	284.5	26.9	34.8
0/100								
1st heating	—	218.8	—	—	—	—	—	—
2nd heating	—	219.2	—	—	—	—	—	—

Isothermal Crystallization Kinetics

The isothermal crystallization kinetics of PPS/PES (100/0–40/60) blends over a temperature range of 240–260°C were analyzed by means of Avrami equation:

$$\chi_c(t)/\chi_c(\infty) = 1 - \exp(-kt^n) \quad (2)$$

where k is the rate constant of crystallization and n is the Avrami exponent, which can be related to the type of nucleation and the geometry of crystal growth. From the intercepts and slopes of the

plots of $\log[-\ln(1 - \chi_c(t)/\chi_c(\infty))]$ versus $\log t$ (Fig. 3), the values of k and n were calculated, respectively; all these values are summarized in Table III. Each curve has a linear portion followed by a gentle roll-off at longer times. The change to a secondary kinetic process is more evident for the PPS/PES blend with high PES content [Fig. 3(d)]. The Avrami exponents are in a range of 3.4–4.2 for both pure and blended PPS, almost independent of crystallization temperature and composition. Their average value is close to four, in agreement with the data of Zheng and Yang,¹³

Table II Nonisothermal Crystallization Parameters for PPS in the Blends with PES

Sample (PPS/PES)	T_{co} (°C)	T_c (°C)	T_{cc} (°C)	$T_{co} - T_{cc}$ (°C)	H_c (J/g)
100/0	253.7	237.5	177.7	76.0	46.9
90/10	251.4	238.8	191.0	60.4	44.9
80/20	250.0	235.6	196.0	54.0	44.4
70/30	249.4	238.1	201.0	48.4	42.9
30/70	249.4	237.7	214.7	34.7	43.6
20/80	256.9	238.4	219.6	37.3	43.4
10/90	253.6	239.6	222.8	30.8	43.0

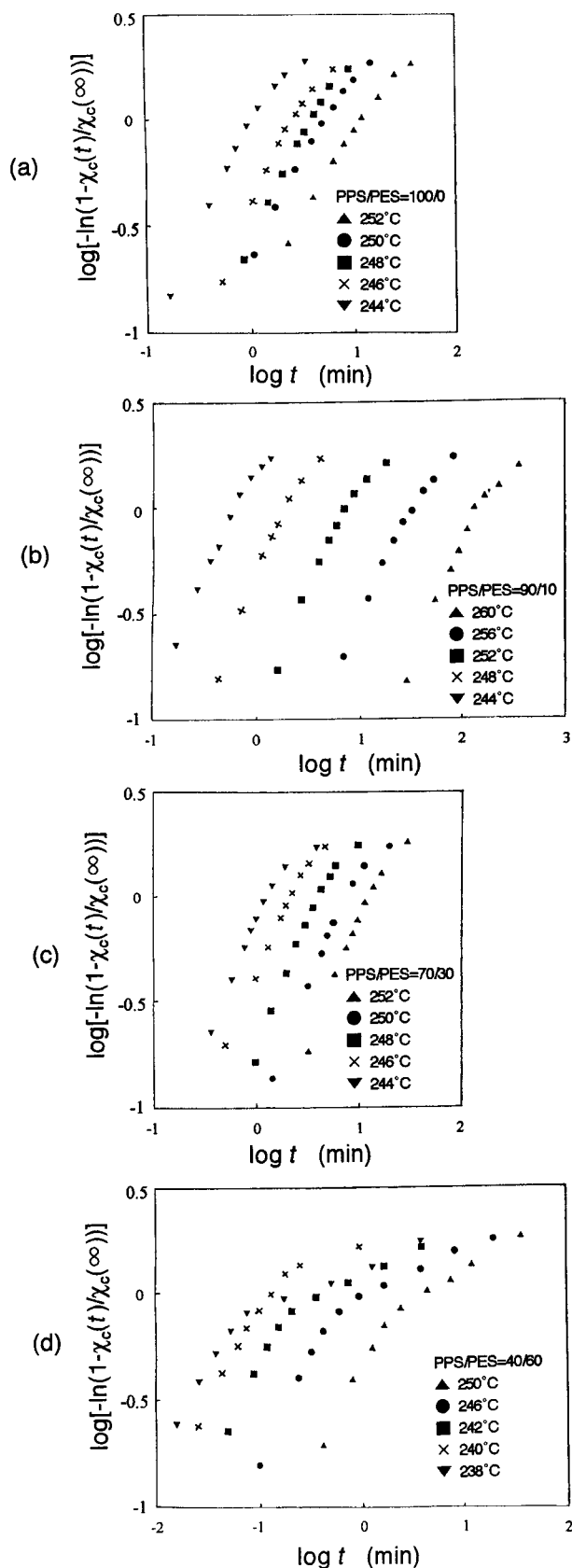


Figure 3 Plots of $\log[-\ln(1 - \chi_c(t)/\chi_c(\infty))]$ versus $\log t$ for PPS/PES blends.

indicating that in the initial crystallization stage, the nucleation process is sporadic, and the growth of crystals is probably spherulitic.¹⁵

The crystallization half times, $t_{1/2}$, the time at which the relative degree of crystallization is 0.5, increase with increasing crystallization temperature. The rate constant k values decrease with increasing crystallization temperature. The value of k for the PPS/PES (90/10) blend is little higher than that of pure PPS compared with the same T_c . When PES content is $\geq 20\%$, k decreased with increasing PES content.

Activation Energy of Crystallization

As the crystallization process is assumed to be thermally activated, the crystallization rate parameter k can be approximately described by an Arrhenius form¹⁶:

$$k^{1/n} = k_0 \exp(-\Delta E/RT) \quad (3)$$

where k_0 is a temperature-independent preexponential factor and ΔE is a total activation energy that consists of the transport activation energy ΔE^* and the nucleation activation energy ΔF . ΔE^* refers to the activation energy required to transport molecular segments across the phase boundary to the crystallization surface. ΔF is the free energy of formation of the critical size crystal nuclei at crystallization temperature T_c . R is the universal gas constant and T is the absolute temperature. The slopes of the Arrhenius plots of $(1/n)\ln k$ versus $1/T$ determine $\Delta E/R$. The values of ΔE for the primary crystallization process were found to be -316 kJ/mol for PPS, -370 kJ/mol for the PPS/PES (90/10) blend, -393 kJ/mol for the PPS/PES (70/30) blend, and -329 kJ/mol for the PPS/PES (40/60) blend. The ΔE of pure PPS is lower than that of the blended PPS. Because ΔE is the energy required to transport molecular segments to the crystallization surface, higher activation energy in the blends suggests that the mobility of the segment is disturbed by the existence of PES in the PPS-rich phase of the blends.

Equilibrium Melting Point

According to Hoffman-Weeks theory,¹⁴ the dependence of the apparent melting temperature T_m on the crystallization temperature (T_c) is given by:

$$T_m = (1 - 1/\gamma)T_m^0 + (1/\gamma)T_c \quad (4)$$

Table III Isothermal Crystallization Parameters for PPS in the Blends with PES

PPS/PES	T_c (°C)	n	k (min ⁻ⁿ)	$t_{1/2}$ (min)	T_m (°C)
100/0	244	3.6	0.97	0.91	276.3
	246	3.7	0.17	1.46	277.3
	248	3.7	0.083	1.77	277.6
	250	3.6	0.058	1.99	278.1
	252	3.4	0.015	3.09	279.1
90/10	244	4.1	3.16	0.69	277.5
	248	3.7	0.35	1.21	277.9
	252	4.0	0.025	2.29	279.7
	256	3.9	0.0015	4.82	281.1
70/30	260	3.9	0.00067	10.70	284.0
	244	4.2	0.94	0.97	276.4
	246	4.0	0.23	1.31	277.5
	248	4.1	0.05	1.90	278.1
	250	4.1	0.013	2.64	279.6
40/60	252	4.2	0.0059	3.11	279.7
	238	3.8	1.7	0.79	274.2
	240	3.9	0.91	0.93	275.4
	242	3.8	0.22	1.35	275.6
	246	3.8	0.03	2.28	277.2
	250	3.9	0.0025	4.23	278.2

where T_m^0 is the equilibrium melting point and γ is the lamellar thickening factor that describes the growth of lamellar thickness during crystallization. Equation (4) shows that T_m and γ can be determined from the intersection with the $T_m = T_c$ line and the slope, respectively, in a Hoffman–Weeks plot of T_m versus T_c . The T_m in the second heating were plotted against T_c (Fig. 4, example plots for PPS/PES 70/30 and 40/60). The values of T_m^0 calculated from the plots are shown in Figure 5. The T_m^0 of pure PPS was 303°C, which is close to the values 303–315°C reported by Lopez and Wilkes¹⁷ and Lovinger et al.¹⁸ The equilibrium melting points of PPS in the blends decreased linearly with increasing PES concentration according to the following equation:

$$T_m^0 = 303 - 16.7w_{\text{PES}} \quad (5)$$

where w_{PES} is the weight fraction of PES in PPS/PES blends. The depression of the equilibrium melting point may be attributed to the partial miscibility of both components.¹⁹ The calculated values of γ were 2.17 for PPS, 2.38, 2.56, and 2.94 for the PPE/PES (90/10, 70/30, and 40/60) blends, respectively. The final lamellar thickness of the PPS crystals in the blends was larger than in the

pure state probably because of a decreased supercooling. It is also known that large γ values can indicate that recrystallization has occurred.²⁰

CONCLUSIONS

PPS/PES blends prepared by melt-mixing showed two glass transition temperatures corresponding to PPS- and PES-rich phases, which increased with increasing PES content, indicating that PPS and PES have some compatibility. Although the crystallization temperature from the melt of the blended PPS was not affected by the composition, the cold crystallization temperature slightly increased with increasing PES content. The melting and crystallization temperature width decreased with increasing PES content. Also, the heats of crystallization and melting of the blended PPS decreased with increasing PES content, indicating that the degree of crystallinity decreased with an increase of PES content. The isothermal crystallization studies over the temperature range of 240–260°C revealed that the crystallization rate constant of PPS increased by blending PPS with 10 wt % PES, and it decreased on further addition of PES. The Avrami exponent n was about 4 independent on blend composition, suggesting the nucleation process is sporadic and the growth of crystals is probably spherulitic. The activation

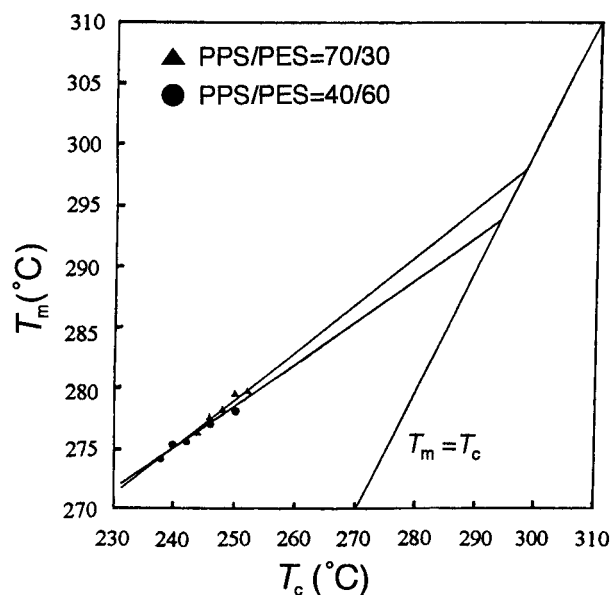


Figure 4 Hoffman–Weeks plots to determine the equilibrium melting temperature of PPS with different PES compositions.

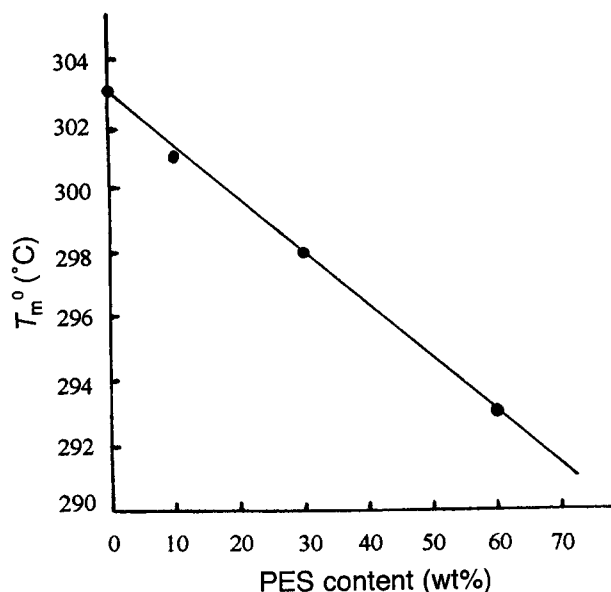


Figure 5 Relationship between equilibrium melting point and PES content for PPS/PES blends.

energy of crystallization increased by blending with PES, suggesting that the mobility of the segment is disturbed by the existence of PES in the PPS-rich phase of the blends. The equilibrium melting point decreased linearly with increasing PES content, indicating the partial miscibility of both components.

This work was financially supported by the National Science Foundation of China (59433072).

REFERENCES

1. Lopez, L. C.; Wilkes, G. L. *J Macromol Sci, Rev Macromol Chem Phys* 1989, C29, 83.
2. Brady, D. G. *J Appl Polym Sci* 1997, 20, 2541.
3. Hsiung, C. M.; Cakmak, M.; White, J. L. *Int Polym Proc* 1990, 5, 109.
4. Jog, J. P.; Nadkarni, V. M. *J Appl Polym Sci* 1985, 30, 997.
5. Desio, G. P.; Rebenfeld, L. *J Appl Polym Sci* 1990, 39, 825.
6. Rebenfeld, L.; Desio, G. P. *J Appl Polym Sci* 1991, 42, 801.
7. Shingankuli, V. L.; Jog, J. P.; Nadkarni, V. M. *J Appl Polym Sci* 1988, 36, 335.
8. Nadkarni, V. M.; Jog, J. P. *J Appl Polym Sci* 1986, 32, 5817.
9. Nadkarni, V. M.; Shingankuli, V. L.; Jog, J. P. *Int Polym Proc* 1987, 2, 53.
10. Radhakrishnan, S.; Joshi, S. G. *Eur Polym J* 1987, 23, 819.
11. Hong, S. M.; Kim, B. C.; Kim, K. U.; Chung, I. J. *Polym J* 1992, 24(8), 727.
12. Jog, J. P.; Shingankuli, V. L.; Nadkarni, V. M. *Polymer* 1993, 34(9), 1966.
13. Zeng, H.; Yang, C. *Acta Polym Sinica* 1989, 5, 538.
14. Hoffman, J. D.; Weeks, J. J. *J Chem Phys* 1962, 37, 1723.
15. Lee, Y.; Porter, R. S. *Macromolecules* 1988, 21, 2770.
16. Cebe, P.; Hong, S.-D. *Polymer* 1986, 27, 1183.
17. Lopez, L. C.; Wilkes, G. L. *Polymer* 1988, 29, 106.
18. Lovinger, A. L.; Davis, D. D.; Padden, F. J., Jr. *Polymer* 1985, 26, 1595.
19. Martuscelli, E. *Polym Eng Sci* 1984, 24(8), 563.
20. Hoffmann, J. D.; Weeks, J. J. *J Res A, Phys Chem* 1962, 66A(1), 13.